CHAPTER (VI)

PETROPHYSICAL MODELING

CHAPTER 6
PETROPHYSICAL MODELING

A petrophysical model is usually designed to facilitate the estimation of an important reservoir parameter that is difficult to be measured or estimated either in laboratory or in the field. The model should be designed to derive this parameter from a conventional or easily measurable other physical parameter. In the present work, the prediction of the permeability is considered to be very important in the oil exploration and during oil field development phases. Theoretical petrophysical models are applied for calculating the permeability from other petrophysical parameters.

6-1. Permeability estimation from a single petrophysical parameter

A simple correlation between permeability and another single petrophysical parameter can only provide a rough approximation with restricted validity. Estimation of permeability by bulk density, porosity, magnetic susceptibility, pore surface to volume ratio, and formation resistivity factor, respectively, is investigated in this section. The data is listed in Table 6-1 of appendix 5.

6-1.1 Determination of permeability from bulk density

The first petrophysical model considers the possibility of permeability prediction for the Bahariya samples from bulk density. The resulting bulk density - permeability relationship

$$Log\ k^* = 18.87 - 8.20\ d_b \qquad (1)$$

Characterized by a coefficient of determination of 0.47. The diagram of the relationship between measured and calculated permeability using equation (1) is shown in Fig 6-1. The bulk density of the non-laminated samples enables a reasonable permeability prediction with most deviations being less than one decade. The reliability of permeability prediction of the laminated samples is worse with some outliers that would considerably overestimate permeability.

6-1.2 Determination of permeability from porosity

The second model aims at the prediction of permeability from porosity. The porosity – permeability relation:

$$Log\ k^* = -3.14 + 0.27\ \Phi \qquad (2)$$

is characterized by a coefficient of determination of 0.63. The relationship between measured and calculated permeability using equation (2) is shown in Fig 6-2.

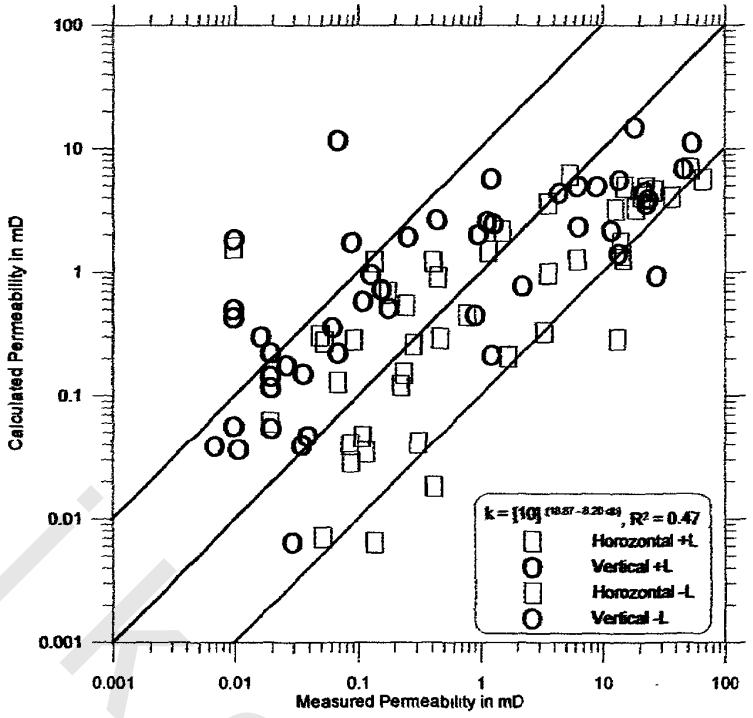

Fig. 6-1 Measured permeability versus predicted permeability from bulk density. 26 data points are used for horizontal laminated, 28 data points are used for vertical laminated, 19 data points are used for horizontal non-laminated and 19 data points are used for vertical non-laminated samples.

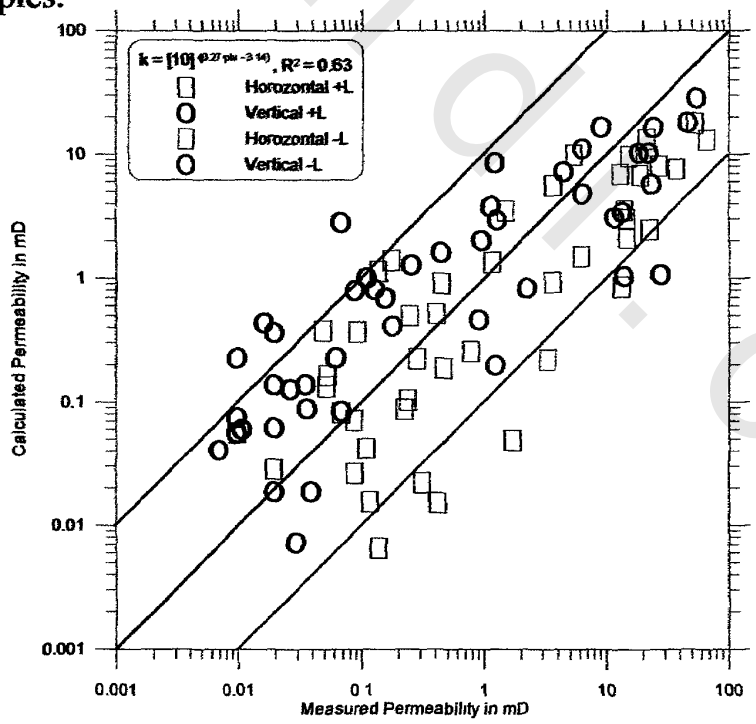

Fig. 6-2 Measured permeability versus predicted permeability from porosity. 26 data points are used for horizontal laminated, 28 data points are used for vertical laminated, 19 data points are used for horizontal non-laminated and 19 data points are used for vertical non-laminated samples.

6-1.3 Determination of permeability from magnetic susceptibility

The third model considers the possibility of permeability prediction from magnetic susceptibility. The magnetic susceptibility - permeability relationship

$$Log\ k^* = 5.21 - 2.77\ log\ \kappa \qquad (3)$$

Characterized by a coefficient of determination of 0.48. The relationship between measured and calculated permeability using equation (3) is shown in Fig 6-3. The use of a unified equation for both laminated and non-laminated sample fails to enable a reliable permeability prediction.

6-1.4 Determination of permeability from pore surface to volume ratio S_{por}

The fourth petrophysical model considers the possibility of prediction of permeability for the Bahariya samples using the pore surface to volume ratio S_{por}. The resulting relationship given by the equation:

$$Log\ k^* = 1.73 - 1.87\ log\ S_{por} \qquad (4)$$

characterized by a coefficient of determination of 0.53. The relationship between measured and calculated permeability using equation (4) is shown in Fig 6-4. The pore surface to volume ratio of the non-laminated samples enables a reasonable permeability prediction with a maximal deviation of one decade. The reliability of permeability prediction of the laminated samples is worse with some outliers that would considerably overestimate permeability.

6-1.5 Determination of permeability from apparent formation resistivity factor

The fifth model aims at the prediction of permeability from apparent formation resistivity factor F'. The apparent formation resistivity factor - permeability relationship is given by the equation:

$$Log\ k^* = 8.07 - 5.02\ log\ F' \qquad (5)$$

with a coefficient of determination of 0.56. The relationship between measured and calculated permeability using equation (5) is shown in Fig 6-5. The use of a unified equation for both laminated and non-laminated sample fails to enable a reliable permeability prediction.

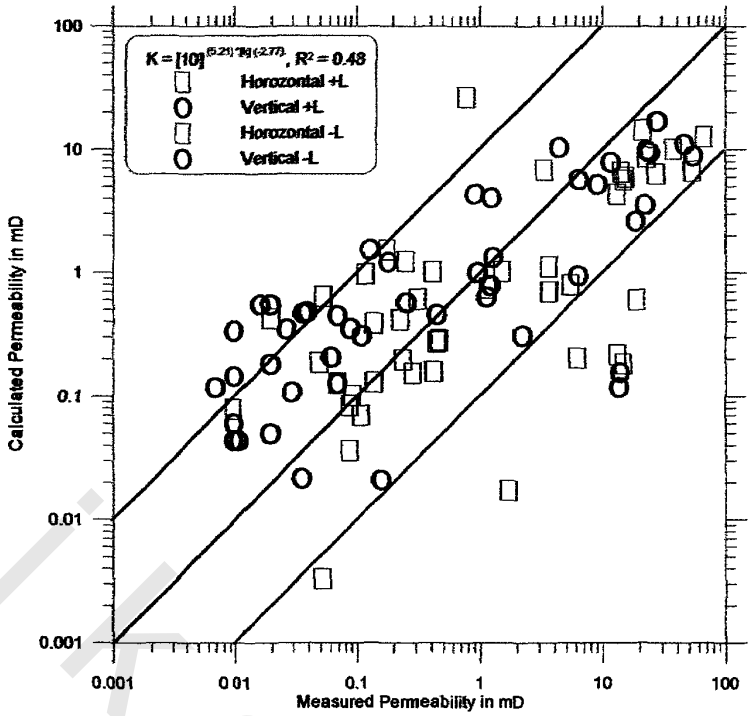

Fig. 6-3 Measured permeability versus predicted permeability from magnetic susceptibility. 26 data points are used for horizontal laminated, 28 data points are used for vertical laminated, 19 data points are used for horizontal non-laminated and 19 data points are used for vertical non-laminated samples.

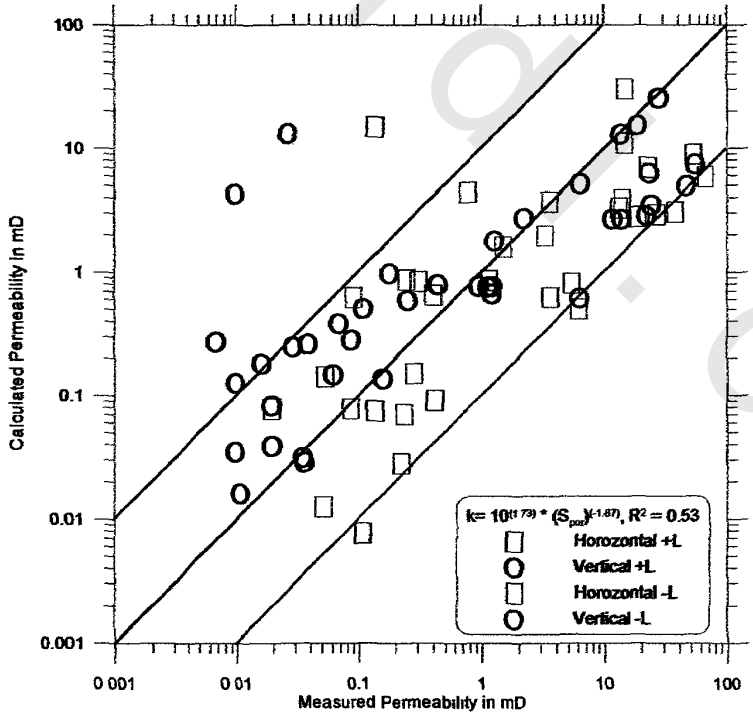

Fig. 6-4 Measured permeability versus predicted permeability from internal surface Spor. 18 data points are used for horizontal laminated, 24 data points are used for vertical laminated, 15 data points are used for horizontal non-laminated and 15 data points are used for vertical non-laminated samples.

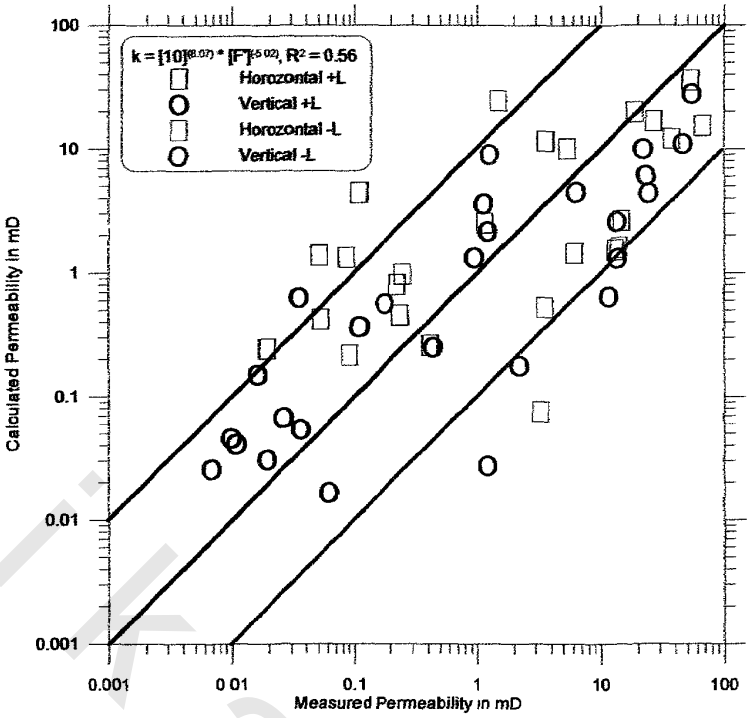

Fig. 6-5 Measured permeability versus predicted permeability from apparent formation resistivity factor. 13 data points are used for horizontal laminated, 14 data points are used for vertical laminated, 13 data points are used for horizontal non-laminated and 13 data points are used for vertical non-laminated samples.

6-1.6 Determination of permeability from true formation resistivity factor

The sixth model considers the possibility of permeability prediction from true formation resistivity factor. The true formation resistivity factor - permeability relationship

$$Log\ k^* = 8.15 - 4.87\ log\ F \qquad (6)$$

results in a reliable coefficient of determination of 0.64. The relationship between measured and calculated permeability using equation (6) is shown in Fig 6-6.

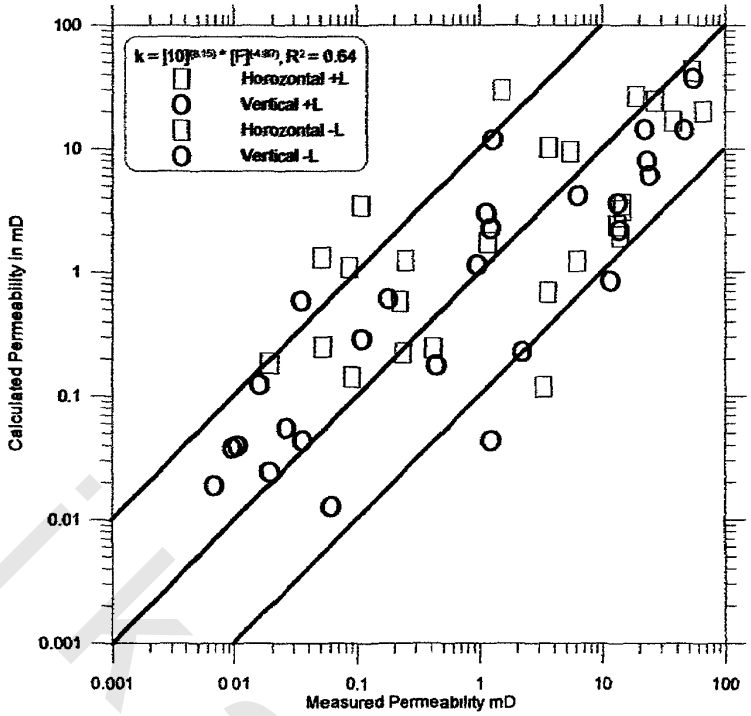

Fig. 6-6 Measured permeability versus predicted permeability from true formation resistivity factor. 13 data points are used for horizontal laminated, 14 data points are used for vertical laminated, 13 data points are used for horizontal non-laminated and 13 data points are used for vertical non-laminated samples.

Table 8 compiles the equations of permeability prediction from a single parameter. Beside the coefficient of determination R^2, the root means square error:

$$RMS = \sqrt{\frac{1}{n}\sum_{i=1}^{n}(\log_{10} k - \log_{10} k_i^*)^2} \qquad (7)$$

and the average deviation:

$$\bar{d} = \frac{1}{n}\sum_{i=1}^{n}|\log_{10} k - \log_{10} k_i^*| \qquad (8)$$

are used to evaluate the quality of permeability prediction.

Table 8: Equations of permeability prediction from a single parameter and statistical data to evaluate the quality of prediction.

Parameters	Equation	n	R^2	RMS	$\bar{d}$
$k^* \sim \Phi$	$Log\ k^* = -3.14 + 0.27\ \Phi$	92	0.63	0.71	0.60
$k^* \sim \kappa$	$Log\ k^* = 5.21 - 2.77\ log\ \kappa$	92	0.48	0.85	0.68
$k^* \sim S_{por}$	$Log\ k^* = 1.73 - 1.87\ log\ S_{por}$	72	0.53	0.81	0.62
$k^* \sim F'$	$Log\ k^* = 8.07 - 5.02\ log\ F'$	53	0.56	0.79	0.67
$k^* \sim F$	$Log\ k^* = 8.15 - 4.87\ log\ F$	53	0.64	0.71	0.59

6-2. Permeability estimation from more than one petrophysical parameter

Considering the model of capillary bundles, it has been shown that at least two parameters are necessary to provide an adequate description of the pore space. One of these quantities is related to porosity as an indicator of the total volume of pore space. The other quantity represents an effective pore size or the pore surface to volume ratio S_{por} that are related to each other. Because the permeability is a property that is controlled by the structure of the pore space, only a set of parameters, which provide a sufficient description of the pore space geometry, can be used to estimate successfully the permeability **(Debschütz and Weller, 2005).** A sample model which was established by **Kozeny (1927)** relates the geometric quantities porosity and the pore surface normalized to the volume of pore space S_{por} from which the permeability can be calculated. Five relations are investigated for permeability estimation by using the statistical software SPSS_16. The relevant data is listed in Table 6-2 of appendix 5.

6-2.1 Determination of permeability from porosity and S_{por}

Using SPSS_16 software, the equation

$$Log\ k^* = -2.83 + 3.70 \log \Phi - 1.06 \log S_{por} \qquad (9)$$

was determined to predict permeability for the Bahariya samples based on pore surface to volume ratio S_{por} (in μm^{-1}) and porosity (in %) data. The calculated multiregression equation is characterized by a coefficient of determination of 0.67. The relationship between measured and calculated permeability using equation (9) is shown in Fig 6-7.

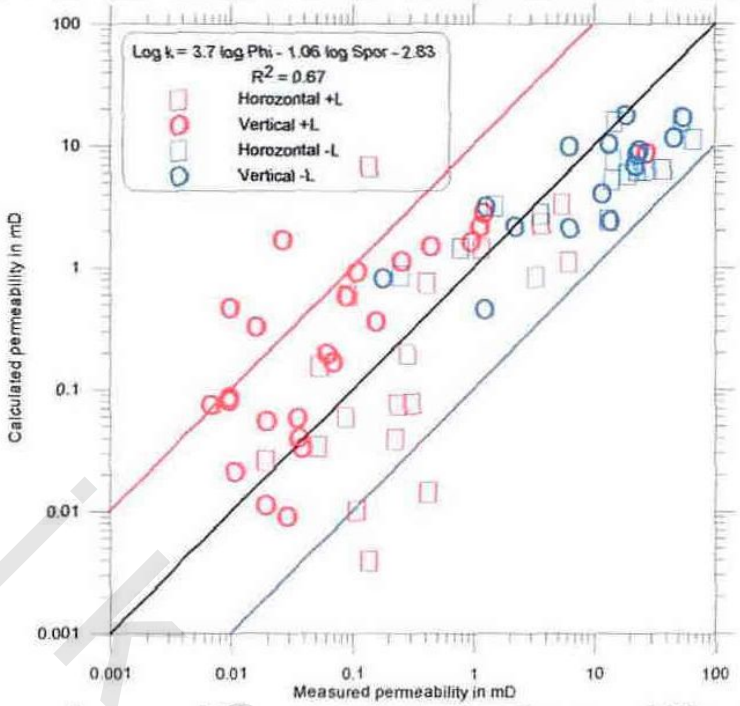

Fig. 6-7 Measured permeability versus predicted permeability from S_{por} and porosity of the Bahariya Formation. 18 data points are used for horizontal laminated, 24 data points are used for vertical laminated, 15 data points are used for horizontal non-laminated and 15 data points are used for vertical non-laminated samples.

6-2.2 Determination of permeability from true formation resistivity factor and S_{por}

The relationship between electrical and hydraulic conductivity can not easily be established **(Mazac et al., 1985).** The porosity is related to formation factor which can be acquired from conventional geoelectrical measurements (see equation 7 in chapter 3). However, no direct method exists to get the pore size or the pore surface to volume ratio from conventional geoelectrical method. Only a complex conductivity measurement, i.e. its imaginary component provides a quantity that can be used to estimate the pore surface to volume ratio. The application of the PaRiS equation **(Pape et al., 1982),** combines formation factor F and S_{por} from which the permeability can be calculated. Using S_{por} (in μm^{-1}) and true formation resistivity factor data the equation

$$Log\ k^* = 7.15 - 1.12\ log\ S_{por} - 3.62\ log\ F \qquad (10)$$

has been determined with a coefficient of determination of 0.79. It should be noted that the original PaRiS equation assumes an exponent of -1 for F and 3.1 for S_{por}. The strong deviation of the exponents in equation (10) might be caused be the anisotropy effects. The relationship between

measured and calculated permeability using equation (10) is shown in Fig 6-8.

6-2.3 Determination of permeability from true formation resistivity factor and imaginary part of the complex conductivity ρ''

Using SPSS_16 software, the equation

$$Log\ k^* = -2.37 - 5.58\ log\ F - 2.59\ log\ \rho'' \quad (11)$$

was determined to predict permeability for the Bahariya samples based on true formation resistivity factor F and imaginary part of the complex conductivity σ'' data. The calculated multiregression equation is characterized by a coefficient of determination of 0.78. The relationship between measured and calculated permeability using equation (11) is shown in Fig 6-9.

6-2.4 Determination of permeability from porosity, S_{por} and true formation resistivity factor

Using SPSS_16 software, the equation

$$\text{Log } k^* = 3.41 + 2.04 \log \Phi - 0.84 \log S_{por} - 2.81 \log F \quad (12)$$

was determined to predict permeability for the Bahariya samples based on porosity (in %), specific internal surface S_{por} (in μm^{-1}) and true formation resistivity factor data. The calculated multiregression equation is characterized by a coefficient of determination of 0.80. The relationship between measured and calculated permeability using equation (12) is shown in Fig 6-10.

6-2.5 Determination of permeability from porosity, S_{por}, ρ'' and true formation resistivity factor

Using SPSS_16 software, the equation

$$\text{Log } k^* = -4.21 + 2.48 \log \Phi - 1.76 \log \rho'' - 0.39 \log S_{por} - 3.56 \log F \quad (13)$$

was determined to predict permeability for the Bahariya samples based on porosity (in %), specific internal surface S_{por} (in μm^{-1}), ρ'' (in mS/m) and true formation resistivity factor data. The calculated multiregression equation is characterized by a coefficient of determination of 0.84. The relationship between measured and calculated permeability using equation (13) is shown in Fig 6-11.

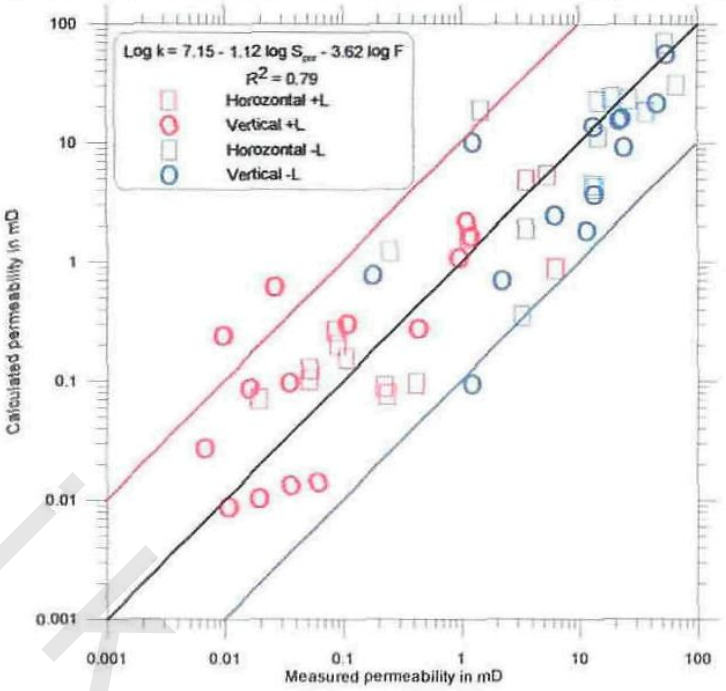

Fig. 6-8 Measured permeability versus predicted permeability from S_{por} and true formation resistivity factor. 13 data points are used for horizontal laminated, 14 data points are used for vertical laminated, 13 data points are used for horizontal non-laminated and 13 data points are used for vertical non-laminated samples.

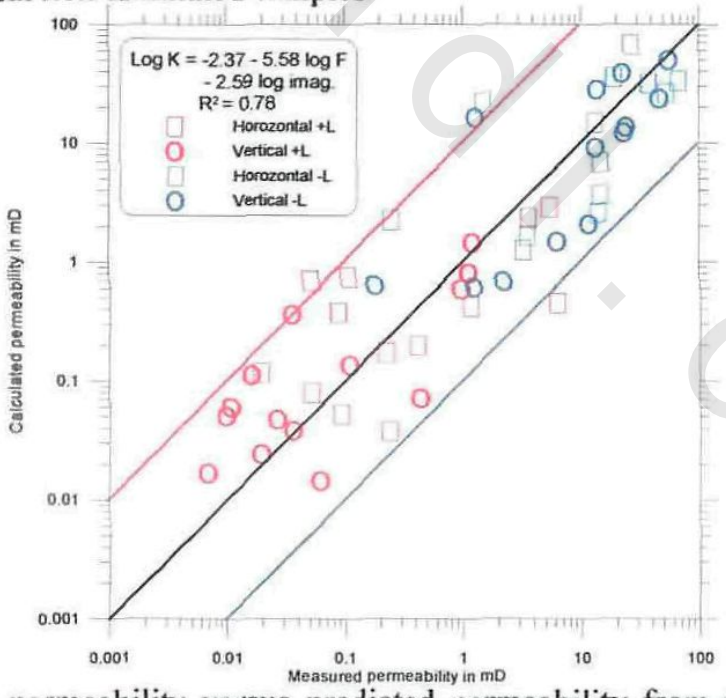

6-9 Measured permeability versus predicted permeability from true formation resistivity factor and imaginary conductivity. 13 data points are used for horizontal laminated, 14 data points are used for vertical laminated, 13 data points are used for horizontal non-laminated and 13 data points are used for vertical non-laminated samples.

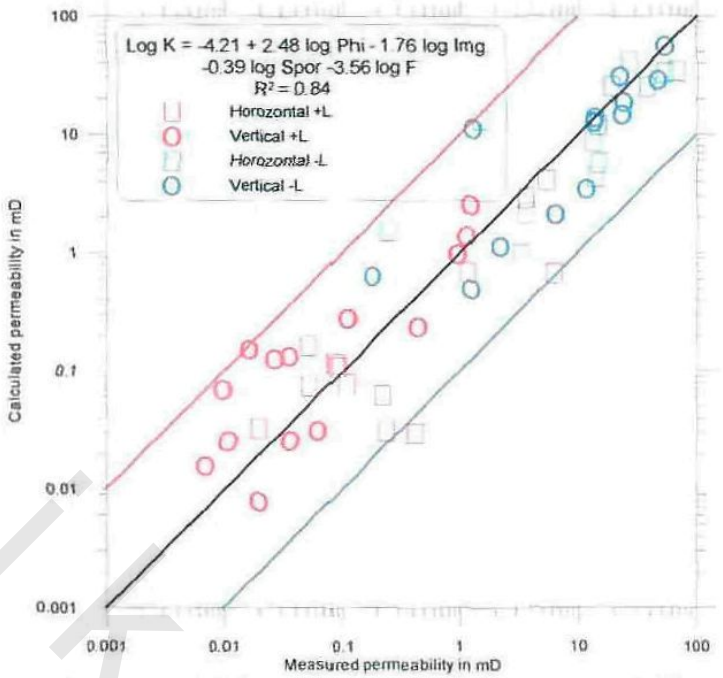

Fig. 6-10 Measured permeability versus predicted permeability from porosity, Spor, and true formation resistivity factor. 13 data points are used for horizontal laminated, 14 data points are used for vertical laminated, 13 data points are used for horizontal non-laminated and 13 data points are used for vertical non-laminated samples.

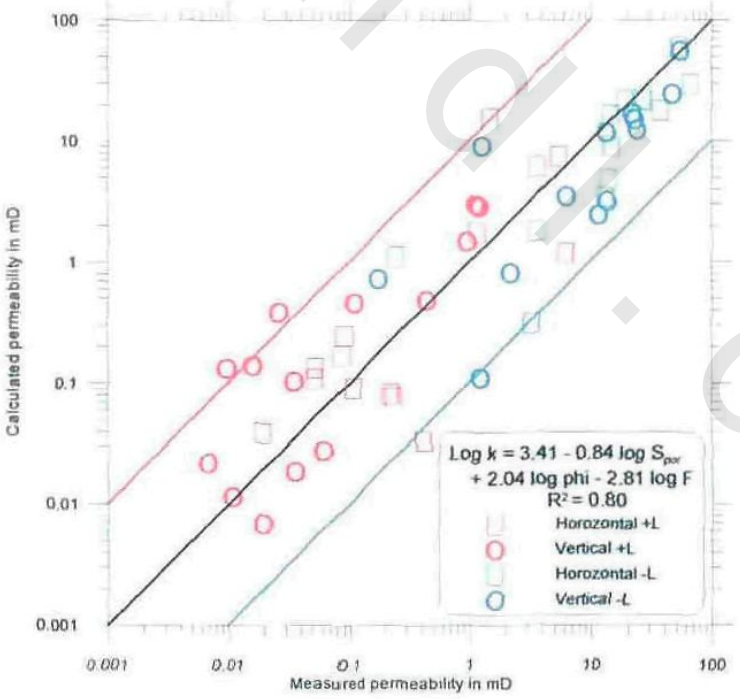

Fig. 6-11 Measured permeability versus predicted permeability from porosity, S_{por}, ρ'' and true formation resistivity factor. 13 data points are used for horizontal laminated, 14 data points are used for vertical laminated, 13 data points are used for horizontal non-laminated and 13 data points are used for vertical non-laminated samples.

Table 9: Equations of permeability prediction from two, three and four parameters and statistical data to evaluate the quality of prediction.

Parameters	Equation	n	R^2	RMS	$\bar{d}$
$k^* \sim (S_{por}$ and $\Phi)$	Log k^* = - 2.83 + 3.70 log Φ - 1.06 log S_{por}	72	0.67	0.68	0.54
$k^* \sim (S_{por}$ and $F)$	Log k^* = 7.15 - 1.12 log S_{por} - 3. 62 log F	53	0.79	0.55	0.44
$k^* \sim (F$ and $\rho'')$	*Log* k^* = -2.37 - 5.58 *log F*- 2.59 *log* ρ''	53	0.78	0.56	0.46
$k^* \sim (\Phi, S_{por}$ and $F)$	Log k^* = 3.41 + 2.04 log Φ - 0.84 log S_{por} – 2.81 log F	53	0.80	0.53	0.43
$k^* \sim (\Phi, S_{por}, \rho''$ and $F)$	Log k^* = -4.21 + 2.48 log Φ -1.76 log ρ'' - 0.39 log S_{por} - 3.56 log F	53	0.84	0.47	0.37